GLOBAL CHANGE BIOLOGY
BIOENERGY

GCB Bioenergy (2015), doi: 10.1111/gcbb.12278

Genetic variation and bidirectional gene flow in the riparian plant *Miscanthus lutarioriparius*, across its endemic range: implications for adaptive potential

JUAN YAN[1], MINGDONG ZHU[1], WEI LIU[2], QIN XU[3], CAIYUN ZHU[2], JIANQIANG LI[1] and TAO SANG[2,3]

[1]*Key Laboratory of Plant Germplasm Enhancement and Specialty Agriculture, Wuhan Botanical Garden, Chinese Academy of Sciences, Wuhan, Hubei 430074, China,* [2]*State Key Laboratory of Systematic and Evolutionary Botany, Institute of Botany, Chinese Academy of Sciences, Beijing 100093, China,* [3]*Key Laboratory of Plant Resources and Beijing Botanical Garden, Institute of Botany, Chinese Academy of Sciences, Beijing 100093, China*

Abstract

Miscanthus lutarioriparius is an endemic species that grows along the middle and lower reaches of the Yangtze River and is a valuable source of germplasm for the development of second-generation energy crops. The plant that propagates via seeds, stem nodes, and rhizomes shows high phenotypic variation and strong local adaptation. Here, we examined the magnitude and spatial distribution of genetic variation in *M. lutarioriparius* across its entire distributional range and tested underlying factors that shaped its genetic variation. Population genetic analyses were conducted on 644 individuals from 25 populations using 16 microsatellite markers. *M. lutarioriparius* exhibited a high level of genetic variation (H_E = 0.682–0.786; A_r = 4.74–8.06) and a low differentiation (F_{ST} = 0.063; D_{est} = 0.153). Of the total genetic variation, 10% was attributed to the differences among populations (df = 24, $P < 0.0001$), whereas 90% was attributed to the differences among individuals (df = 619, $P \leq 0.0001$). Genetic diversity did not differ significantly across longitudes and did not increase in the populations growing downstream of the Yangtze River. However, significant associations were found between genetic differentiation and spatial distance. Six genetic discontinuities were identified, which mostly distributed among downstream populations. We conclude that anthropogenic factors and landscape features both contributed to shaping the pattern of gene flow in *M. lutarioriparius*, including long-distance bidirectional dispersal. Our results explain the genetic basis of the high degree of adaptability in *M. lutarioriparius* and identify potential sources of new germplasm for the domestication of this potential second-generation energy crop.

Keywords: bidirectional migration, genetic connectivity, genetic diversity, microsatellite, *Miscanthus lutarioriparius*, Yangtze River

Received 23 March 2015 and accepted 1 May 2015

Introduction

Analysis of population connectivity plays an important role in protecting endangered species and managing economically important species, which was defined as the degree to gene flow affecting evolutionary processes within populations (Hedgecock *et al.*, 2007; Lowe & Allendorf, 2010). Likewise, plants' genetic diversity can contribute significantly to their adaptability to environmental changes such as global warming, drought, and urbanization (Hughes *et al.*, 2008; Medrano & Herrera, 2008; Markert *et al.*, 2010; Verhoeven *et al.*, 2011; Wang, 2012; Raymond *et al.*, 2013). Therefore, understanding gene-flow patterns and genetic diversity could facilitate conservation practices and exploitation of genetic resources for utilization.

Traditionally, methods like Wright's *F*ST-statistic (1969) and Slatkin's private allele have been used to analyze gene flow indirectly by measuring the spatial distribution of gene frequencies over time. However, these methods are inadequate to capture short-term changes in movement patterns, including populations that are not in equilibrium (Abdo *et al.*, 2004; Paetkau *et al.*, 2004). With advanced molecular tools, a landscape genetic approach was developed to study the interaction between landscape features and gene flow, which enables characterizing population genetic processes of plants inhabiting river systems, for instance (Manel *et al.*, 2003; Pollux *et al.*, 2009; Murphy *et al.*, 2010; Andrew *et al.*, 2012; Manel & Holderegger, 2013; Rico

Correspondence: Jianqiang Li, tel. +86 27 87510330, fax: +86 27 87510251, e-mail: lijq@wbgcas.cn; Tao Sang, tel. +86 10 62836172, fax: +86 10 62590843, e-mail: sang@ibcas.ac.cn

et al., 2014). This approach can be used to explain the spatial genetic variation patterns in a species by charactering the clines, isolation by distance, and genetic boundaries to gene flow among populations and by relating theses genetic structures to landscape features (Meeuwig et al., 2010; Song et al., 2013; Wei et al., 2013; Taylor & Hoffman, 2014).

River systems provide an opportunity to study the interactions between genetic variation and eco-geographical factors of hydrochloric (i.e., water dispersing) plants due to the unidirectional flow of water (Bergl & Vigilant, 2007; Honnay et al., 2010; Orsini et al., 2013; Catford et al., 2014). Generally, hydrological dispersion results in the increased genetic diversity along the river systems by seeds and clones from flood damaged stands-washing the steams and rhizomes downstream. This hypothesis was confirmed for *Myricaria laxiflora* in the Three Gorges Valley of the Yangtze River (Liu et al., 2006), *Sparganium emersum* in a stretch of Nier River (Pollux et al., 2009) and *Heliconia metallica* along a stretch of river in the Amazon lowlands (Schleuning et al., 2011), but other studies have not found the expected pattern (Chen et al., 2009; Wei et al., 2013). Thus, understanding the patterns of gene flow and population connectivity of the riparian plant is valuable for studying the genetic variation and adaptive potential of the species.

Miscanthus lutarioriparius is a perennial grass that primarily grows in wetlands along the middle and lower reaches of the Yangtze River (29–31°N; 112–119°E). It was recognized as a separate species from *Miscanthus sacchariflorus* according to the thicker and taller tillers and vigorous growth along seasonally flooded river banks and lake shores in central China (Chen & Renvoize, 2006), despite some remaining taxonomic controversy (Sun et al., 2010). *Miscanthus lutarioriparius* can propagate clonally by rhizomes and sexually through outcrossing. The hairy caryopsis seeds are capable of long-distance dispersal through biotic and abiotic dispersal agents. Because of its commercial utilization by the paper industry, the propagules (seeds and rhizomes) are migrated long distances by humans through water and land transportation; especially, *Miscanthus* species are considered to be promising second-generation energy crops (Jørgensen & Schwarz, 2000; Clifton-Brown et al., 2004; Somerville et al., 2010; Sang & Zhu, 2011; Clark et al., 2014). Some recent studies of *Miscanthus* genetic diversity were carried out, including *Miscanthus* × *giganteus*, *M. sacchariflorus*, and *Miscanthus sinensis* (Chae et al., 2014; Clark et al., 2014, 2015; Głowacka et al., 2015). To date, little is known about the genetic diversity of *M. lutarioriparius* across its distribution range, although it is particularly promising energy crop with high biomass production and water-use efficiency, and strong ability to grow in the stressful environments (Sang, 2011; Liu et al., 2012, 2014; Yan et al., 2012, 2015; Liu & Sang, 2013; Mi et al., 2014; Xu et al., 2015).

We used 16 highly polymorphic microsatellite markers to analyze 25 *M. lutarioriparius* populations across its native distribution range. The aims of our study were to examine the magnitude and spatial distribution of genetic variation and identify the gene-flow patterns in *M. lutarioriparius*. For these purposes, we first estimated the genetic diversity and population connectivity of the surveyed populations. Based on landscape features and eco-geographical patterns, we predicted that *M. lutarioriparius* is subject to substantial genetic recombination and bidirectional migration. Our study sheds light on the genetic structure and gene flow of a riparian plant and identifies populations which may be particularly valuable sources of new germplasm for energy crop development.

Materials and methods

Sample collection

From 2008 to 2010, a total of 644 of *M. lutarioriparius* individuals were collected from 25 populations in the middle and lower reaches of Yangtze River (Fig. 1), which covered the entire native range of the species. Nineteen populations were collected along the Yangtze River, and six populations were collected in land. From each plant, cleaned plant leaves (2 × 5 cm) were sampled every 10–20 m across linear transects and immediately stored in plastic bags filled with silica gel for subsequent DNA extraction.

Microsatellite genotyping

Plant genomic DNA was isolated from approx. 1 g of dried leaves using a modified cetyltrimethy lammonium bromide (CTAB) protocol (Doyle & Doyle, 1987). DNA quality was tested on 0.8% agarose gels. After measuring DNA concentration with an Eppendorf BioPhotometer, samples were diluted to 5 ng μL^{-1}. Twenty-five individuals (one per population) were chosen for microsatellite primer selection. A total of 35 microsatellite loci (Hung et al., 2009; Zhou et al., 2011, 2013) were tested in the study, and sixteen microsatellite loci were amplified by PCR for further analysis (Table S1, Supporting information). PCRs were carried out in a GeneAmp PCR System 9700 (Applied Biosystems, Foster City, CA, USA) with 10 μL volumes containing 1* PCR buffer, 1.5 mM MgCl2, 200 μM each dNTP, 0.4 μM fluorescently labeled forward primer (FAM and HEX), 0.4 μM reverse primer, and 0.5 U Expand High-Fidelity Polymerase. PCR conditions were as follows: 94 °C for 5 min, 32 cycles of 94 °C for 50 s, 45 s of annealing at 54–60 °C, 1 min of elongation at 72 °C, a final extension step of 72 °C for 10 min. Microsatellite products were run on an ABI 3730XL automated sequencer at the Sangon Biotech and geno-

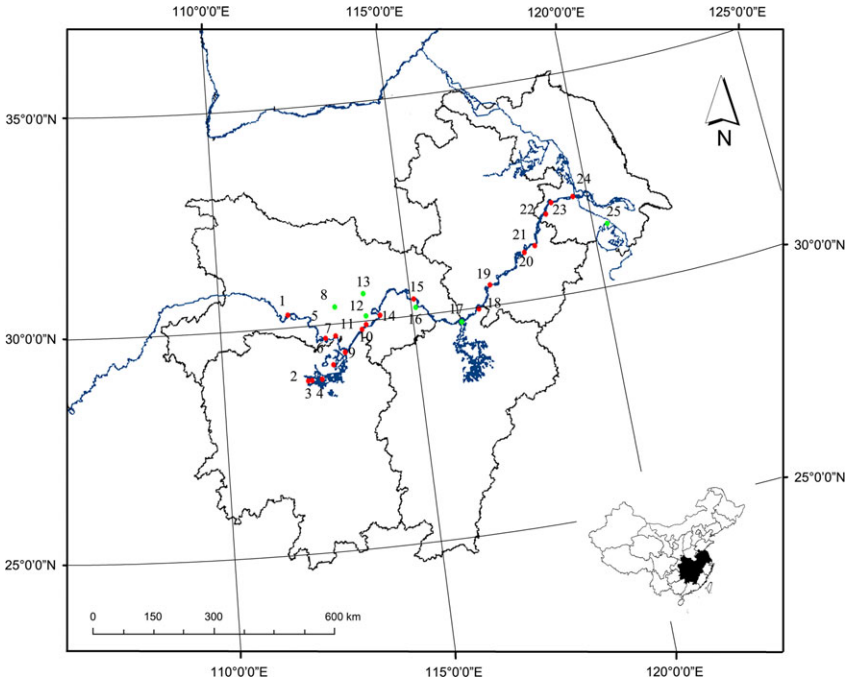

Fig. 1 Locations of the sampled *Miscanthus lutarioriparius* populations across its distribution range. Population identities correspond to codes in Table 1. Red dots indicate samples along the Yangtze River, and green dots indicate samples from land in the middle and lower Yangtze River.

typed using GeneMarker 1.95. Based on the results of flow cytometry (Li *et al*., 2013) and the peaks of reads, we eliminated the probable tetraploid individuals. A total of 644 individuals were included in the dataset for analysis (ranged from 12 to 33 individuals and mean 25.8 individuals/population). Accessions were scored at each locus for two alleles, corresponding to the two largest peaks shown by GeneMarker 1.95. Potential scoring errors and null alleles were checked by MICRO-CHECKER v2.2.3 (Van Oosterhout *et al*., 2004).

Data analysis

Genetic diversity analysis

We used GenAlEx 6.0 (Peakall & Smouse, 2006) to identify the clonal structure of each population. Repeating genotypes within populations were excluded from all further analyses. Next, we used GENEPOP v4.0.11 (Raymond & Rousset, 1995) to test whether loci and populations were in Hardy–Weinberg equilibrium (HWE), using Fisher's exact test (Guo & Thompson, 1992), and ran a Markov chain for 10 000 steps following 10 000 dememorization steps for a standard Bonferroni correction. We also used FSTAT version 2.9.3 (Goudet, 1995) to analyze linkage disequilibria (LD) for all pairs of loci in each population, the number of alleles (A), observed heterozygosity (H_O), genetic diversity (H_E), fixation index (F_{IS}) averaged across loci for each populations, as well as genetic differentiation among populations (F_{ST}) and allelic richness (A_r). To test the unidirectional genetic diversity hypothesis, observed heterozygosity (H_O) and allele richness (A_r) of the populations were correlated with longitude of the population origin using a Spearman rank correction with SPSS 16.0 (SPSS Inc., Chicago, IL, USA). The Yangtze River is generally divided into three sections: the upper reaches, from the river's source to Yichang (more than 4500 km long), the middle reaches, from Yichang to Hukou (29.71°N, 115.97°E), (950 km long), and the lower reaches, from Hukou to the river mouth at about 930 km long (Yang *et al*., 2006). Based on the geographic boundaries of the Yangtze River, we divided populations as upstream and downstream with the boundary point at longitude 115.7°E and calculated the correlation between genetic variation (H_O and A_r) and longitude using SPSS 16.0.

Genetic differentiation and population structure

Genetic structure of the species was investigated using a number of approaches: (i) analysis of molecular variance (AMOVA) and *F*-statistics, (ii) PCoA, and (iii) nonhierarchical Bayesian clustering. First, AMOVA was performed on all individuals using GenAlEx 6.0 (Peakall & Smouse, 2006). Pairwise *F*-statistics (Weir & Cockerham, 1984) were calculated to estimate the

genetic differentiation between populations, based on the differences in allele frequencies. Their significance levels were estimated with 6000 permutations as implemented in FSTAT 2.9.3 (Goudet, 1995). Because F_{ST} is dependent on marker variability (Hedrick, 2005; Jost, 2008), we additionally calculated pairwise D_{est} (Jost, 2008), an alternative measure of genetic differentiation, using the program SMOGD (Crawford, 2010). Second, we performed principal coordinate analysis (PCoA) at the different levels based on Nei's genetic distance (N_A, Nei *et al*., 1983). Third, to explore the genetic groups within the samples, nonhierarchical Bayesian clustering was performed using the program STRUCTURE 2.3.4 (Pritchard *et al*., 2000). The program was used with a burn-in of 100 000 replicates, followed by 1000 000 replicates of the Markov chain Monte Carlo (MCMC) simulation, with the admixture model and the assumption of correlated allele frequencies among populations. Three iterations were performed for each value of K from 1 to 15. The output was interpreted with Structure Harvester (Earl & vonHoldt, 2012) using the methods of Pritchard *et al.* (2000) and Evanno *et al.* (2005) and visualized by DISTRUCT v. 1.1 (Rosenberg, 2004).

Population genetic structure landscape

Mantel tests were performed in IBD 2.0 (Bohonak, 2002) with 10 000 permutations between pairwise genetic distance ($[F_{ST}/(1-F_{ST})]$; $[D_{est}/(1-D_{est})]$) and geographic distance (km) in all populations. Additionally, spatial autocorrelation analysis was performed on genetic distances between all individuals over multiple populations using GenAlEx 6.0 (Smouse & Peakall, 1999; Peakall & Smouse, 2006). Multiple distance classes were tested to have the best chance of identifying spatial genetic structure, and these analyses were repeated at variable distance classes and even sample classes. Permutation and bootstrap tests were conducted with 10 000 replicates in each case. Barrier 2.2 (Manni *et al*., 2004) implementing Monmonier's algorithm was used to identify the geographical boundaries associated with genetic differentiation among populations. Barriers calculated geographic discontinuities in the genetic structure according to a multilocus genetic differentiation (F_{ST}; Weir & Cockerham, 1984), along with their geographical coordinates for each population. Analyses were conducted both for each of the sixteen loci separately, and also for the complete dataset. Only barriers supported by at least half of the loci (i.e., ≥8 loci) were allowed as 'consensus barriers'. The analysis of individual loci estimated how many loci supported each identified barrier.

Gene-flow and population history

We used GENECLASS 2.0 (Piry *et al*., 2004) to perform the assignment test with the Bayesian method (Rannala & Mountain, 1997) and to detect the first-generation migrants among populations with the frequency-based method (Paetkau *et al*., 1995). The assignment test was used to assign or exclude the possible origins of individuals in reference populations, with 1 000 000 simulations and an alpha level of 0.01. The first-generation migrants among populations were conducted with Monte Carlo resampling of 1000 individuals and a threshold of 0.01, which identified the immigrant individuals that were not born in the population. The migration rate could indicate the gene flow at a particular time, but it may not accurately reflect long-term patterns of gene flow (Slatkin, 1987). F_{ST} and private allele methods were used to estimate historical rates of gene flow (Nm). F_{ST} method was executed according to Wright's island model of population genetic structure ($F_{ST} \approx 1/(1 + 4Nm)$) (Slatkin & Barton, 1989). The private allele method was used to estimate the effective numbers of migrants per generation using GENEPOP v4.0.11 (Raymond & Rousset, 1995). BOTTLENECK 1.2.02 (Piry *et al*., 1999) was used to assess whether a population exhibited a significant bottleneck. The program assumes that the population after a bottleneck shows a larger heterozygosity than what is expected under the mutation-drift equilibrium. We conducted the Wilcoxon sign-rank test with a two-phase mutational model (TPM, Di Rienzo *et al*., 1994) and two other mutational models (stepwise mutation model and infinite allele model). The TPM was set at 90% single-step mutations, assuming a conservative variance among multiple steps of 10. With the expectation that rapid reduction in allelic diversity under a bottleneck would cause a mode-shift distortion (Luikart *et al*., 1998), the allele frequency distribution test was also performed to examine frequencies of all alleles in populations and compare them with the distribution expected at mutation-drift equilibrium.

Results

Defining genotypes and estimating genetic diversity of Miscanthus lutarioriparius

Among the multilocus genotypes, three pairs of clones were identified: plant #3 was similar to plant #4, #28 was similar to plant #29 (both within LU8), and plant #1 was similar to #2 in LU16. We calculated the maximal clone sizes of the species with 13.153 m and 21.213 m in LU8 and LU16, respectively. The subsequent analyses were performed on the 641 genetically distinct individuals. As allele frequencies per locus per population were not

consistent in their pattern for other loci or populations, all sixteen loci were used for subsequent analyses. A total of 203 alleles were identified, ranging from 5 (C-1) to 19 (F-1), with an average of 12.68 alleles per locus (Table S1). The mean number of alleles within populations ranged from 5.125 (LU8) to 8.875 (LU10) (Table 1). The mean observed heterozygosity (H_O) and expected heterozygosity (H_E) per population were 0.866 and 0.766, respectively (Table 1). The smallest and the highest H_E values were observed in the LU8 and LU13 populations, which were growing along the tributary of the Yangtze River. After excluding populations with less than 20 individuals, allelic richness ranged from 4.74 (LU8) to 8.06 (LU10) (Table 1). The average value of the fixation index was very low (mean: −0.161, range: −0.36 to −0.07; Table 1), suggesting that *M. lutarioriparius* is strictly outcrossing, and our samples were derived from randomly mating populations (panmixis).

Significant departures ($P < 0.05$) from Hardy–Weinberg equilibriums were detected in 170 of the 400 population-loci comparisons. According to all loci and populations, this result may arise from the low frequency of null alleles or small sampling effects. Genotypic disequilibrium was tested in 120 pairs of loci combinations by Fisher's exact test. No pairs of loci showed a significant disequilibrium after Bonferroni correction, which revealed that loci were physically unlinked and statistically independent.

Spatial variation in genetic diversity was examined across the species' range. No significant spatial patterns in H_O and A_r among populations at longitude were detected (H_O: $r = -0.005$, $P = 0.998$; A_r: $r = -0.140$, $P = 0.544$; Fig. 2). Upstream populations (longitude breakpoint at 115.7°E) showed a comparable average H_E (0.744) and A_r (7.323) as downstream population (0.748 and 6.996, respectively). Linear correlations revealed a nonsignificant increase for H_O ($r = 0.160$, $P = 0.553$; Fig. 2a) and A_r ($r = 0.192$, $P = 0.476$; Fig. 2b) in upstream population. In downstream populations, genetic diversity showed a trend for positive correlation with H_O (Fig. 2a) and for negative correlation with A_r (Fig. 2b).

Genetic differentiation and population structure

Table S2 shows a matrix of the pairwise population differentiation estimated by F_{ST} (below the diagonal)

Table 1 Summary measures of genetic diversity for each population, including the location of populations, sample size (*N*), average of allele numbers (*A*), observed heterozygosity (H_O), expected heterozygosity (H_E), allelic richness (A_r), and inbreeding coefficient (F_{IS}). Bold populations are from the land and others are along Yangtze River

Populations	Latitude (N)	Longitude (E)	N	*A*	H_O	H_E	A_r	F_{IS}
LU1	30°24′09.6″	111°41′46.7″	31	8.125	0.843	0.743	7.42	−0.134
LU2	28°53′29.4″	112°01′32.0″	29	8	0.842	0.706	7.3	−0.193
LU3	28°53′24.5″	112°06′49.2″	30	7.6875	0.879	0.741	6.93	−0.185
LU4	28°52′13.2″	112°22′26.3″	27	7.625	0.824	0.752	7.16	−0.095
LU5	29°46′27.7″	112°36′11.7″	30	8.5	0.902	0.744	7.54	−0.212
LU6	29°09′51.8″	112°44′06.3″	29	8.5	0.831	0.725	7.59	−0.146
LU7	29°47′51.4″	112°51′40.1″	29	8.5	0.823	0.744	7.81	−0.105
LU8	**30°27′04.8″**	**112°56′02.3″**	**33**	5.125	**0.927**	**0.682**	4.74	**−0.36**
LU9	29°24′48.8″	113°04′05.1″	30	8.375	0.903	0.748	7.48	−0.207
LU10	29°52′02.1″	113°34′44.8″	30	8.875	0.841	0.752	8.06	−0.118
LU11	29°57′36.6″	113°40′48.8″	30	7.4375	0.824	0.726	6.86	−0.133
LU12	**30°09′13.3″**	**113°42′32.3″**	**24**	8.0625	**0.907**	**0.777**	7.71	**−0.17**
LU13	**30°39′48.9″**	**113°43′35.7″**	**30**	8.6875	**0.921**	**0.786**	7.9	**−0.17**
LU14	30°08′24.9″	114°04′18.3″	30	8.5	0.925	0.774	7.69	−0.194
LU15	30°23′56.9″	115°00′26.6″	23	8.0625	0.882	0.754	7.75	−0.169
LU16	**30°13′06.8″**	**115°01′08.3″**	**30**	7.75	**0.817**	**0.764**	7.23	**−0.07**
LU17	**29°44′38.65″**	**116°09′55.49″**	**12**	6.437	**0.867**	**0.756**	–	**−0.15**
LU18	29°59′25.88″	116°39′08.05″	28	7.687	0.825	0.726	7	−0.135
LU19	30°29′38.40″	117°00′07.34″	29	8.25	0.898	0.7665	7.51	−0.171
LU20	31°07′05.29″	118°00′05.44″	22	6.812	0.812	0.728	6.65	−0.115
LU21	31°14′28.10″	118°17′15.66″	30	8.375	0.913	0.765	7.65	−0.193
LU22	31°55′43.05″	118°39′39.40″	11	6.625	0.876	0.758	–	−0.155
LU23	32°09′59.47″	118°49′46.83″	21	6.312	0.82	0.715	6.17	−0.146
LU24	32°14′35.96″	119°24′44.20″	14	6.812	0.843	0.774	–	−0.089
LU25	**31°32′19.00″**	**120°13′23.19″**	**12**	6.125	**0.908**	**0.745**	–	**−0.22**

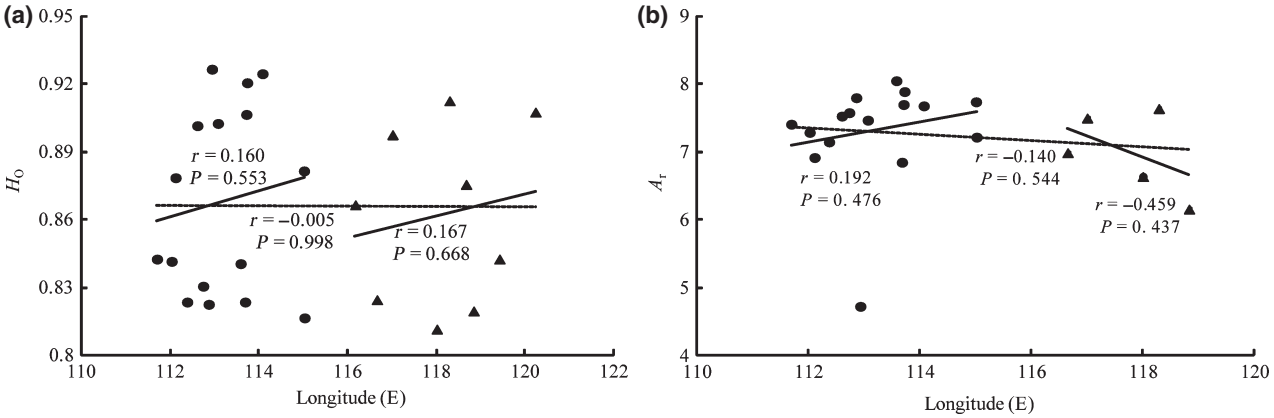

Fig. 2 Geographic patterns of genetic diversity across the species' range (a) H_O and (b) A_r. Piecewise linear correlation identified at the boundary point (115.7°E) of the upstream (●) and downstream (▲) of Yantgze River.

Table 2 The analysis of molecular variance (AMOVA) of *Miscanthus lutarioriparius* across the species range

Source	df	SS	MS	Est. Var.	Var.%	Φ_{pt}	*P*
Among Pops	24	941.964	39.248	1.139	10%		
Within Pops	616	6177.400	9.980	9.980	90%	0.102	0.010
Total	641	7119.364	49.228	11.119			

and by D_{est} (above the diagonal). A total of 283 pairwise comparisons were significant ($P < 0.05$) for genetic differentiation between populations after correction for multiple tests. LU3, LU8, LU11, LU14, LU18, LU19, LU20, LU23 were significantly differentiated from all populations after correction for multiple tests ($P \leq 0.01$). The nonsignificant differentiation was primarily found for comparisons within LU17 and LU22 (Table S2), which may be due to the limited sample sizes for the two populations. Levels of pairwise population differentiation were low and moderate, ranging between 0.0037 and 0.1122 (mean $F_{ST} \pm$ SEM: 0.063 ± 0.008). Consistent with these results, values of Jost's D_{est} were similar (0–0.1993) between all populations (mean $D_{est} \pm$ SEM: 0.153 ± 0.02). The AMOVA showed that the overall population differentiation was low, but significant ($\Phi_{pt} = 0.102$, $P = 0.01$). Of the total genetic variation partitioned in the 25 *M. lutarioriparius* populations, 10% was attributed to the differences among populations (df = 24, $P < 0.0001$), whereas 90% was attributed to the differences among individuals (df = 619, $P \leq 0.0001$) (Table 2).

STRUCTURE software with the Bayesian model was used to estimate the number of homogeneous gene pools (*K*) and confirmed a constant increase in ln P(*K*) from $K = 1$ to $K = 15$ with low variance across replicate runs. Evaluation of the most appropriate *K* value following the procedure by Evanno *et al.* (2005) found two clear peaks for ΔK, at $K = 2$ and 4, suggesting that a model with two gene pools captures a major split, with substantially additional resolution provided under a model with $K = 4$ (Fig. 3a). Considering the inspection of Q (proportional membership) values for $K = 2$ with high levels of admixture, the $K = 4$ model was used as prior information. The four clusters of individuals clearly separated these collecting locations into stable gene pools. Some individuals from downstream locations (LU17-25) had more similar alleles than others from the upstream populations, with fewer cases in the opposite direction (Fig. 3b). Further investigation using hierarchical STRUCTURE analyses revealed that LU8 was split into two genetically distinguishable groups, one that had similar alleles with other populations and one that was specific for this population, suggesting the presence of a barrier that partially cut off LU8 from the other populations.

Spatial genetic structure

There was a significant association between genetic differentiation and geographic distance across the total range, although only a small proportion of the genetic variance was explained by geography (F_{ST}: $r = 0.3907$, $P = 0.0002$; D_{est}: $r = 0.2947$, $P = 0.004$; Fig. 4). The characterization of spatial genetic structure at the individual level, as calculated with GenAlex, revealed a consistent pattern with IBD, where the pairwise kinship coefficients decreased with distance. Positive kinship coefficients (*r*) were found in the range of 60 m, with an x-

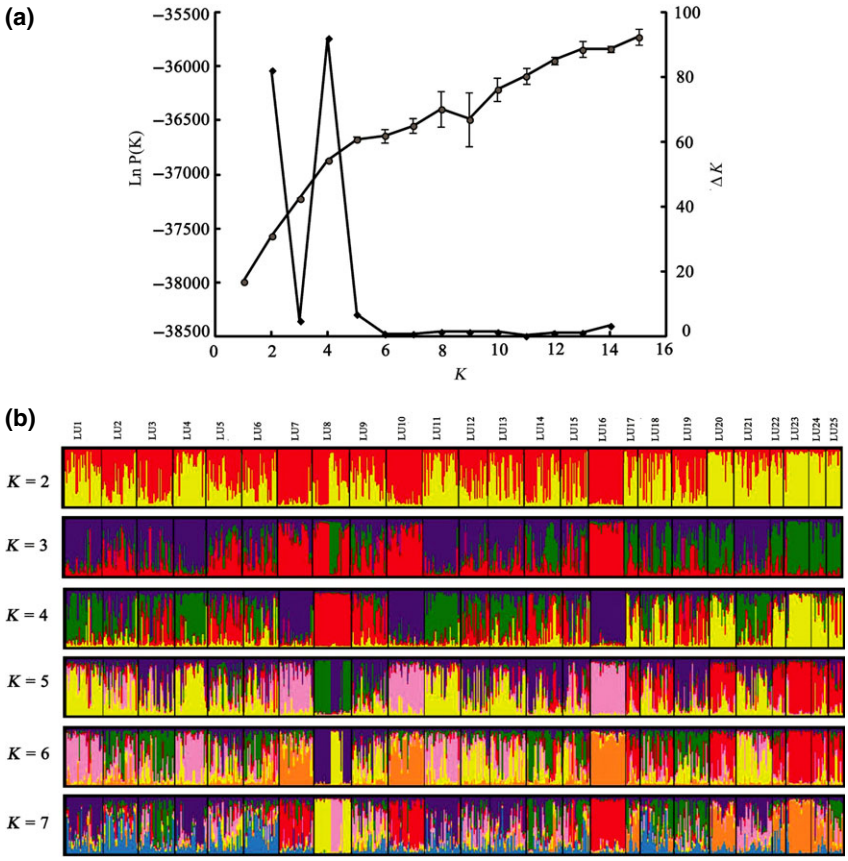

Fig. 3 Estimations of the number of gene pools across the *M. lutarioriparius* distribution range. (a) The number of Bayesian clusters (*K*) among 25 populations using Ln P(*K*) (●; Pritchard *et al*., 2000) and Δ*K* (■; Evanno *et al*., 2005); (b) population structure inferred from admixture analysis from *K* = 2 to *K* = 7 clusters identified in Bayesian analyses. A thin vertical line represents individuals that were separated into K-colored segments. Black lines separate individuals from different populations (labeled above).

intercept of 78 m (Fig. 5a). The kinship coefficients were highest at the first distance class and rapidly decreased from there. At the range of 20 m, *r* value was the highest in the LU2 (*r* = 0.325). Similarly, autocorrelation in all sites was positive up to about 60 m, and, with the exception of LU3, LU18, LU23, LU24, and LU25, with *r* values below zero (data not shown). In Fig. 5b, the correlation values were positive and significant up to 150 m and significantly negative at 300 m, with an x-intercept of 190.8 m. Figure 5a showed an oscillation of high and low autocorrelation, indicating a mosaic of higher and lower densities at different scales.

Barrier analysis

Analyses using Barrier 2.2 identified six main genetic discontinuities based on pairwise F_{ST} values (Fig. 6a). The first barrier, computed on the F_{ST} distance matrix, divides LU23 from adjacent populations (LU22 and LU24) and was supported completely by 15 loci. The results showed that the thickness of the barrier decreased from the LU22 to LU24, thus suggesting that the genetic barrier was strong only between LU22 and LU23. The second break and third break separated LU21 and LU22, and LU19 and LU20 with a support of 11 loci. The fourth break separated samples of LU16 from LU15 and LU17, which was wholly supported by 10 loci. This break was in agreement with other analysis, such as STRUCTURE, which splits these populations into upstream and downstream. A fifth break and sixth break were detected by 9 loci, of which the former separated LU8 from other neighboring samples and the latter separated LU24 from LU25. Other genetic discontinuities identified by barrier 2.2 did not meet the majority rule criterion of being supported by at least 50% of all loci and therefore was not considered further. Overall, the six geographical barriers significantly and stably separated the downstream populations into distinct gene pools. When considering genetic structure based on the PCoA performed on allelic frequencies, a similar pattern was found. PCoA explained 77.73% of the total gene variation, on the basis of the first dimension

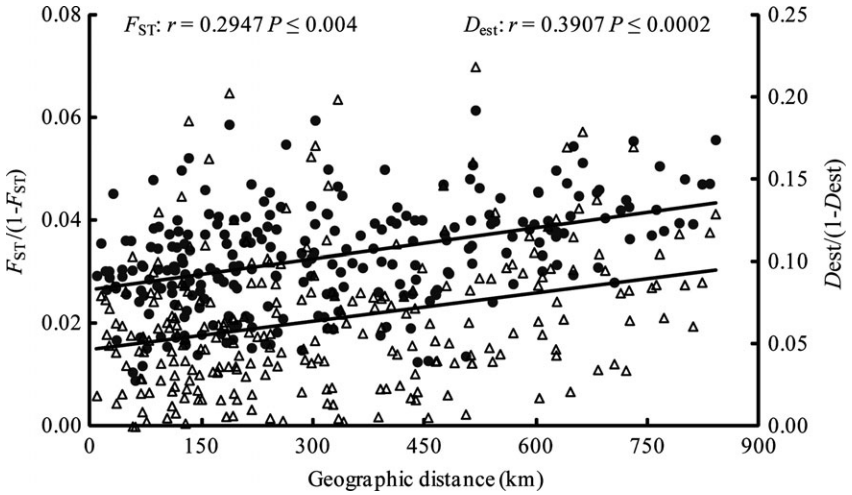

Fig. 4 Mantel test of correlation of genetic distance with geographic distance for populations of *M. lutarioriparius*. Pairwise values between populations are calculated by F_{ST} (●;Weir & Cockerham, 1984) and D_{est} (○; Jost, 2008).

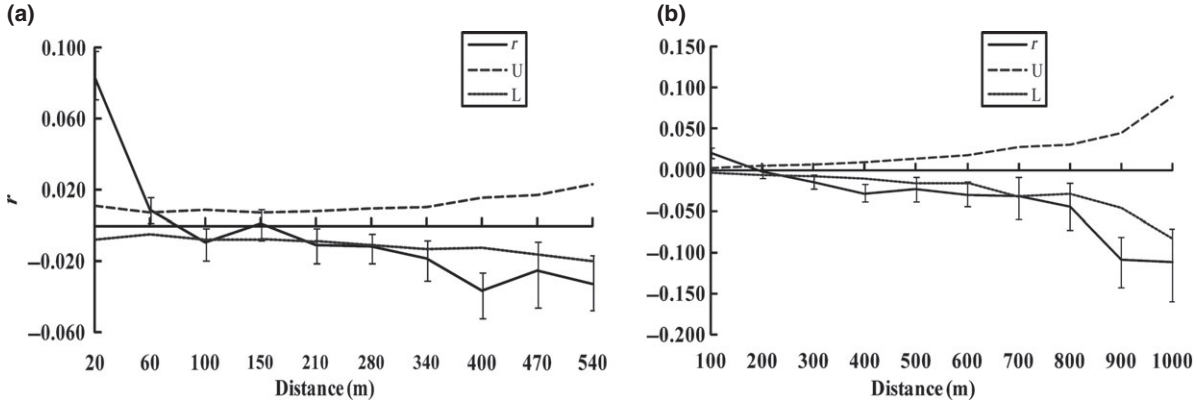

Fig. 5 Correlogram for the spatial pattern of *M. lutarioriparius* based on multiple populations in the program GenAlex 6.0. (a) 540 m (b) 1000 m. *r* indicates correlation coefficient. U and L indicate upper and lower limits by 95% confidence interval of the null hypothesis of no spatial structure.

(34.05%, $P < 0.001$), the second dimension (24.07%, $P < 0.001$), and the third dimension (19.61%, $P < 0.001$) (Fig. 6b).

Gene-flow and population history

An assignment test showed that individuals from their population of origin were 54.3% or higher in all the natural populations, and 4.5% or less of the individuals were assigned to their nearest origin population. Additionally, 37.3% or less of the individuals was assigned to the other populations. Some 3.9% or less of the individuals were not assigned to any of the populations sampled (Fig. S1). Thirty first-generation immigrants were detected, of which sixteen had migrated up from the downstream populations and fourteen had migrated down from upstream (Table 3). Based on F_{ST}- and private allele methods, historical gene flow was estimated at 3.718 and 2.862 among *M. lutarioriparius* populations, respectively (Table S1).

We tested for signatures of recent bottlenecks for these populations and found significant heterozygosity excess in all populations, except LU6 under the IAM. Interestingly enough, none of the populations showed significant heterozygosity excess under TPM and SMM. The allele frequency distribution tests did not show any shifts in allele frequency distribution shapes (Table 4).

Discussion

Genetic diversity and adaptation

For a species that is endemic in wetlands of the Yangtze River, *M. lutarioriparius* exhibited a higher level of

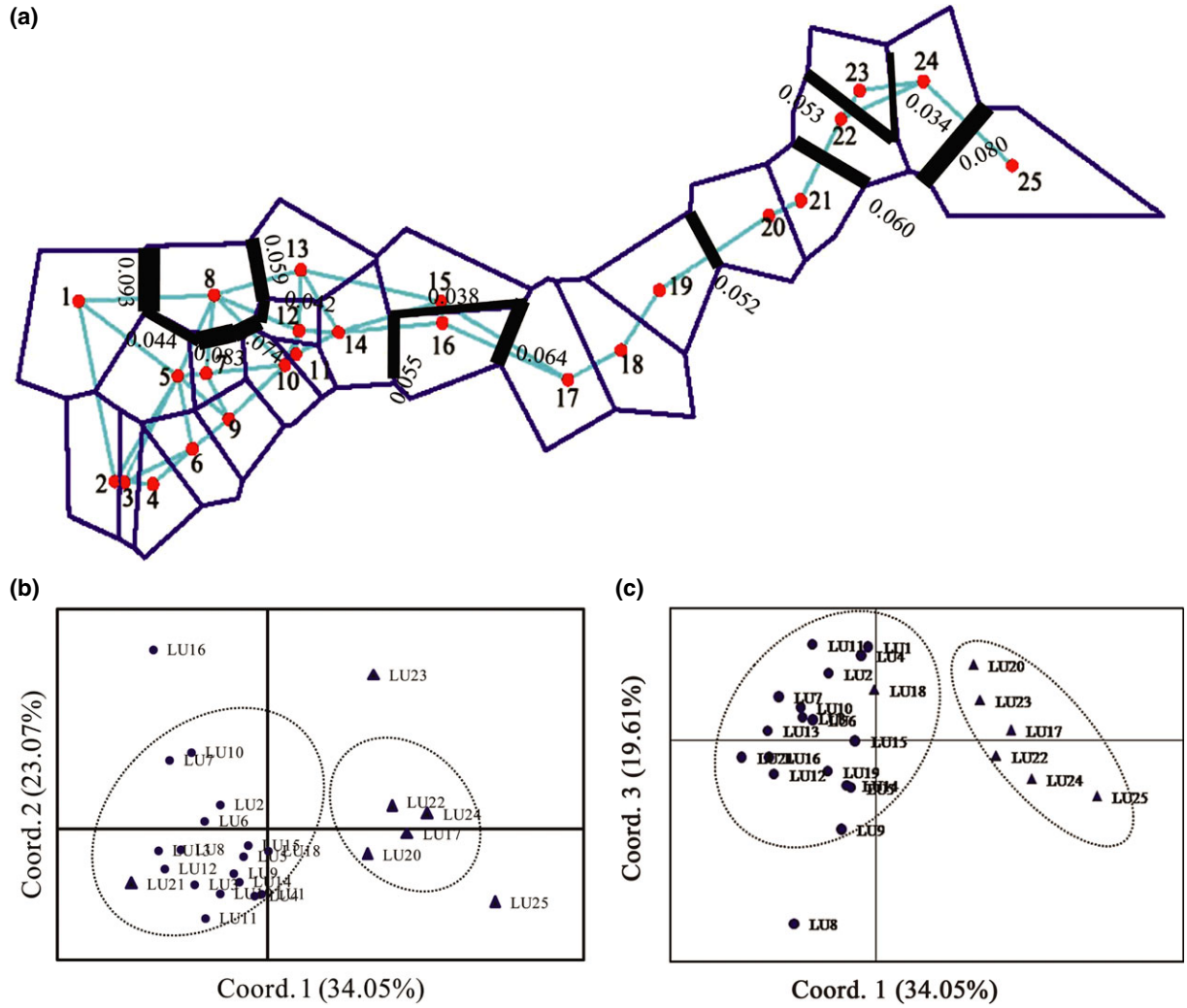

Fig. 6 Genetic landscape of *M. lutarioriparius*. (a) Major discontinuities in gene flow suggested by BARRIER using consensus barriers (>8 loci), with rank order given in letters. The A was supported by 15 loci, the B barrier by 11 loci, the C by 10 loci, and the D by 9 loci. Additional barriers were identified, but were weakly supported (<8 loci) and were largely restricted to the downstream of the species' range. (b) Nonmetric multiddimensional scaling ordination among upsteam (●) and downstream (▲) based on Nei's genetic distance (D_A; Nei *et al*., 1983).

genetic variation across its distribution range (H_E = 0.682–0.786; A_r = 4.74–8.06; Tables 1 and S1) compared to *Myricaria laxiflora* and *Zizania latifolia* within the same habitat and distributing range (Liu *et al*., 2006; Chen *et al*., 2012). However, the genetic diversity was comparable with the riparian pioneer tree species *Populus nigra* along the Drôme River (France), which had similar dispersal mechanisms (Imbert & Lefèvre, 2003). Generally, pioneer species tend to be less subdivided and more genetically diverse than species that establish more slowly (Vrijenhoek, 2010). Therefore, combined with the growing characters and genetic diversity of the species, we inferred that *M. lutarioriparius* might have established quickly and recently. Notably, we found that the clonal reproduction of the species was not as widespread as commonly assumed. We found only three clonal genotypes in 644 samples, with rhizomes spreading no more than 25 m. Above all, *M. lutarioriparius* showed a considerable level of genetic diversity, which may be explained by the specific traits of the species, including perenniality, self-incompatibility (F_{IS} < 0), weak clonal reproduction, and various modes of distribution.

Genetic diversity plays an important role in the adaptation capabilities of species and their susceptibility to environmental changes (Raymond *et al*., 2013). Measurements of the relationship between genetic variation and adaptive traits have already been conducted in a number of species, which showed that species with high

Table 3 First-generation immigrants and the direction of migration among 25 populations across the distributional range; populations divided as upstream and downstream at longitude 115.7°E

Individual	Migrated from	Direction of migration	*P* value
LU1 no.10	LU11	Downstream	0.01
LU1 no.20	LU13	Downstream	0.001
LU2 no.5	LU6	Downstream	0.008
LU2 no.14	LU6	Downstream	0.001
LU3 no.4	LU13	Downstream	0.001
LU5 no.1	LU19	Downstream	0.003
LU5 no.4	LU24	Downstream	0.006
LU6 no.19	LU15	Downstream	0.009
LU7 no.14	LU10	Downstream	0.003
LU8 no.23	LU9	Downstream	0
LU8 no.24	LU9	Downstream	0.003
LU9 no.21	LU5	Upstream	0.005
LU10 no.10	LU7	Upstream	0.007
LU10 no.11	LU3	Upstream	0.009
LU11 no.23	LU1	Upstream	0.007
LU12 no.24	LU9	Upstream	0.002
LU14 no.9	LU15	Downstream	0.008
LU15 no.9	LU20	Downstream	0.007
LU15 no.22	LU22	Downstream	0.003
LU16 no.21	LU7	Upstream	0.004
LU17 no.1	LU22	Downstream	0
LU19 no.16	LU1	Upstream	0.007
LU19 no.21	LU4	Upstream	0.009
LU20 no.3	LU4	Upstream	0.002
LU21 no.30	LU19	Downstream	0.001
LU22 no.2	LU17	Upstream	0.002
LU22 no.4	LU20	Upstream	0.005
LU23 no.2	LU5	Upstream	0
LU23 no.3	LU6	Upstream	0.005
LU25 no.3	LU15	Upstream	0.004

Table 4 Wilcoxon tests for recent bottlenecks in the program BOTTLENECK. IAM (infinite allele model), TPM (two-phase mutational model), SMM (stepwise mutation model); all with a normal L-shaped distribution

	IAM	TPM	SMM
LU1	0.00134	0.7057	0.1297
LU2	0.00629	0.56189	0.1753
LU3	0.0001	0.97995	0.3225
LU4	0.00008	0.2114	0.93988
LU5	0.00011	0.4637	0.0832
LU6	0.07391	0.2312	0.0576
LU7	0.00011	0.78195	0.19281
LU8	0.00002	0.00919	0.05768
LU9	0.00002	0.82089	0.46375
LU10	0.00025	0.93988	0.37546
LU11	0.00029	0.70572	0.52817
LU12	0.00008	0.15806	0.66855
LU13	0.00001	0.09344	1
LU14	0.00021	0.97995	0.27444
LU15	0.00029	1	0.25223
LU16	0.00003	0.01825	0.11667
LU17	0.00029	0.46375	0.82089
LU18	0.00134	0.11667	0.01309
LU19	0.00003	0.97995	0.27444
LU20	0.0005	0.19281	0.66855
LU21	0.00004	0.78195	0.66855
LU22	0.01099	0.56189	0.17535
LU23	0.00029	1	0.46375
LU24	0.00107	0.56189	0.97995
LU25	0.0005	0.25223	0.4332

level of genetic diversity and gene flow have higher phenotypic plasticity (Reed & Frankham, 2003; Ghalambor *et al.*, 2007; Gruber *et al.*, 2013). For example, LU8 with lower genetic variation had a weaker adaptability than other populations in the Loess Plateau, and other populations with higher genetic variation had a stronger adaptability to establish in a new environment (Yan *et al.*, 2012). *M. lutarioriparius* shows a high level of genetic diversity, which is consistent with its capability to adapt to the stressful environments.

Geographic pattern of genetic variation

It is generally assumed that the effective population size and genetic variation increases in downstream populations of riparian species due to the movement of seeds and propagules with the water. However, *M. lutarioriparius* does not seem to follow this pattern. Genetic variation was not associated with the longitude of the collection sites. Furthermore, genetic variation was not different between the upstream and downstream environment of the Yangtze River when taking the traditional longitude breakpoint (115.7°E) based on hydrological characteristics. Generally, clinal variation in allelic frequencies results from founder events or spatially restricted gene flow (Vasemägi, 2006; Hasselman *et al.*, 2013). The observed pattern therefore indicates that *M. lutarioriparius* populations have enough gene flow and are in gene-flow-drift equilibrium. Genetic variation slightly decreased in downstream populations compared with upstream, which may be due to differences in landscape architecture, anthropogenic factors such as farming and general habitat suitability.

Genetic differentiation and gene flow

Life style, mating system and mode of seed dispersal are important adaptive traits that affect genetic differentiation among populations (Mable & Adam, 2007; Vähä *et al.*, 2007; Yan *et al.*, 2009). For instance, perennial, outcrossing, bird-dispersed, and wind-disseminated seeds

and pollen generally have less genetic differentiation than annual, self-crossing species with gravity and insect-mediated dispersal. *M. lutarioriparius* exhibited low genetic differentiation among populations across the geographic range in this study, as supported by the AMOVA results with only 10% variation existing among populations ($P = 0.01$). Assignment analysis revealed that close to 50% of the sampled individuals might derive from other populations. Similarly, the analysis of gene-flow history also indicated a high rate of migration. Gene flow for *M. lutarioriparius* was estimated to be higher than in other terrestrial plants such as *Vouacapoua americana* and *Castanopsis sclerophylla* (Dutech *et al*., 2004; Wang *et al*., 2011). The low genetic differentiation and high level of gene flow are likely the result of a combination of factors, including a perennial life style, self-incompatibility, strong dispersal, and anthropogenic displacement.

It is interesting to note that immigration was higher in upstream populations than in downstream populations. The result may be due to several factors; firstly, the interseasonal flood in upstream region may have enabled propagules (fruits, seeds, or rhizomes) to disperse by floating and establishing in wetland after floods. Secondly, Dongting lake, as a typical estuary wetland, is one of the important stopovers of migration route for eastern birds (Deng & Wang, 2000), which may have increased the dispersal of caryopses. Finally, commercial activity with the plant was higher in the upstream regions, which may have increased anthropogenic gene flow.

Spatial genetic structure, population history, and population connectivity

The detection of four genetically distinguishable groups among the 25 populations by Bayesian clustering should be considered conservative, as this method has limited power under scenarios involving weak genetic differentiation (Faubet *et al*., 2007; Faubet & Gaggiotti, 2008). Despite the low population differentiation, we found a general pattern of IBD at the scale of kilometers, which indicates either ongoing gene flow or a recent colonization process (Slatkin, 1993). Additionally, kinship coefficients between individuals were positive at a scale of hundreds of meters and only disrupted over distances of around 200 m by spatial autocorrelation analysis, a widespread tool for estimating genetic structure and patterns of gene flow. The correlation between genetic distance and geographic distance is consistent with population mixing by migratory movements. The significant isolation-by-distance patterns and the spatial autocorrelation patterns are indicative that the populations were close to equilibrium. Moreover, the significant isolation of distance allowed us to reject the infinite island model of migration, suggesting that the species was not subjected to bottleneck effects.

Detecting genetic discontinuities is necessary to understand dispersal restrictions and to identify factors which influence population structure (Manel *et al*., 2003; Meeuwig *et al*., 2010). Several genetic discontinuities were detected across the distribution range of *M. lutarioriparius* (Fig. 6a), despite the high dispersal capacity of the species. PCoAs further supported the pattern (Fig. 6b). We found that barriers to individual migrations largely occurred in regions with high anthropogenic activities (e.g., dam and urban development). The three major genetic borders (LU8, LU16, and LU23) correspond with physical barriers, such as LU8 along the villages, and LU16 and LU23 along the Yangtze River levees. Similar patterns have been found in other plant species. Small irrigation diversion dams, for instance, were found to restrict the interactions of *Oncorhynchus mykiss* populations (Weigel *et al*., 2013).

In conclusion, this study assessed genetic variation and gene flow across *M. lutarioriparius* populations. Our results provide a genetic basis for the adaptation potential of the species that was revealed by some previous studies (Yan *et al*., 2012, 2015; Xu *et al*., 2015). *M. lutarioriparius* has a high level of genetic diversity and a low level of genetic differentiation, both of which can enhance the capacity of plants to adapt to changing environments. Furthermore, the species shows long-distance, bidirectional gene flow with unequal dispersal among populations in the middle and lower Yangtze River, probably as a result of anthropogenic activities and landscape features. The high level of gene flow that in turn enriched the genetic variation of the species should be beneficial for the domestication and cultivation of the energy crop on marginal land with unfavorable and often stressful conditions.

Acknowledgements

We thank Matthias Erb for revising the manuscript and providing helpful scientific input. We thank Zhiqiang Sun, Xinwei Li, Zuling Ning, Fan Luo, Nature Reserve Region of East Dongting Lake, P. R. China for help this project in the process of sampling. This study was supported by the National Natural Science Foundation of China (NSFC91131902), the Knowledge Innovation Program of the Chinese Academy of Sciences (KSCX2-EX-QR-1), and the Screening and Demonstration of High-Resistant Bioenergy Plants in Marginal Land (2013BAD22B02).

Data archiving

Data deposited in the Dryad repository: doi:10.5061/dryad.bh274.

References

Abdo Z, Crandall KA, Joyce P (2004) Evaluating the performance of likelihood methods for detecting population structure and migration. *Molecular Ecology*, **13**, 837–851.

Andrew RL, Ostevik KL, Ebert DP, Rieseberg LH (2012) Adaptation with gene flow across the landscape in a dune sunflower. *Molecular Ecology*, **21**, 2078–2091.

Bergl RA, Vigilant L (2007) Genetic analysis reveals population structure and recent migration within the highly fragmented range of the Cross River gorilla (*Gorilla gorilla diehli*). *Molecular Ecology*, **16**, 501–516.

Bohonak AJ (2002) IBD (isolation by distance): A program for analyses of isolation by distance. *Journal of Heredity*, **93**, 153–154.

Catford JA, Morris WK, Vesk PA, Gippel CJ, Downes BJ (2014) Species and environmental characteristics point to flow regulation and drought as drivers of riparian plant invasion. *Diversity and Distribution*, **20**, 1084–1096.

Chae WB, Hong SJ, Gifford JM, Rayburn AL, Sacks EJ, Juvik JA (2014) Plant morphology, genome size, and SSR markers differentiate five distinct taxonomic groups among accessions in the genus *Miscanthus*. *Global Change Biology Bioenergy*, **6**, 646–660.

Chen SL, Renvoize SA (2006) *Miscanthus*. In: *Flora of China* (eds Wu ZY, Raven PH, Hong DY), pp. 581–583. Science Press & Missouri Botanical Garden Press, Beijing & St Louis.

Chen YY, Li XL, Yin LY, Cheng Y, Li W (2009) Genetic diversity and migration patterns of the aquatic macrophyte *Potamogeton malaianus* in a potamo-lacustrine system. *Freshwater Biology*, **54**, 1178–1188.

Chen YY, Chu HJ, Liu H, Liu YL (2012) Abundant genetic diversity of the wild rice *Zizania latifolia* in central China revealed by microsatellites. *Annals of Applied Biology*, **161**, 192–201.

Clark LV, Brummer JE, Glowacka K *et al.* (2014) A footprint of past climate change on the diversity and population structure of *Miscanthus sinensis*. *Annals of Botany*, **114**, 97–107.

Clark LV, Stewart JR, Nishiwaki A *et al.* (2015) Genetic structure of *Miscanthus sinensis* and *Miscanthus sacchariflorus* in Japan indicates a gradient of bidirectional but asymmetric introgression. *Journal of Experimental Botany*, doi:10.1093/jxb/eru511.

Clifton-Brown JC, Stampfl PF, Jones MB (2004) *Miscanthus* biomass production for energy in Europe and its potential contribution to decreasing fossil fuel carbon emissions. *Global Change Biology*, **10**, 509–518.

Crawford NG (2010) SMOGD: software for the measurement of genetic diversity. *Molecular Ecology Resources*, **10**, 556–557.

Deng X, Wang B (2000) Structure and diversity of winter bird community in Southern Dongting Lake. *Sichuan Journal of Zoology*, **19**, 236–238.

Di Rienzo A, Peterson AC, Garza JC, Valdes AM, Slatkin M, Freimer NB (1994) Mutational processes of simple-sequence repeat loci in human-populations. *Proceedings of the National Academy of Sciences of the United States of America*, **91**, 3166–3170.

Doyle JJ, Doyle JL (1987) A rapid DNA isolation procedure for small quantities of fresh leaf tissue. *Phytochemical Bulletin*, **19**, 11–15.

Dutech C, Joly HI, Jarne P (2004) Gene flow, historical population dynamics and genetic diversity within French Guianan populations of a rainforest tree species, *Vouacapoua americana*. *Heredity*, **92**, 69–77.

Earl D, vonHoldt B (2012) STRUCTURE HARVESTER: a website and program for visualizing STRUCTURE output and implementing the Evanno method. *Conservation Genetics Resources*, **4**, 359–361.

Evanno G, Regnaut S, Goudet J (2005) Detecting the number of clusters of individuals using the software STRUCTURE: a simulation study. *Molecular Ecology*, **14**, 2611–2620.

Faubet P, Gaggiotti OE (2008) A new bayesian method to identify the environmental factors that influence recent migration. *Genetics*, **178**, 1491–1504.

Faubet P, Waples RS, Gaggiotti OE (2007) Evaluating the performance of a multilocus Bayesian method for the estimation of migration rates. *Molecular Ecology*, **16**, 1149–1166.

Ghalambor CK, McKay JK, Carroll SP, Reznick DN (2007) Adaptive versus nonadaptive phenotypic plasticity and the potential for contemporary adaptation in new environments. *Functional Ecology*, **21**, 394–407.

Głowacka K, Clark LV, Adhikari S *et al.* (2015) Genetic variation in *Miscanthus* × *giganteus* and the importance of estimating genetic distance thresholds for differentiating clones. *Global Change Biology Bioenergy*, **7**, 386–404.

Goudet J (1995) FSTAT (Version 1.2): A computer program to calculate *F*-statistics. *Journal of Heredity*, **86**, 485–486.

Gruber K, Schöning C, Otte M, Kinuthia W, Hasselmann M (2013) Distinct subspecies or phenotypic plasticity? Genetic and morphological differentiation of mountain honey bees in East Africa. *Ecology & Evolution*, **3**, 3204–3218.

Guo SW, Thompson EA (1992) Performing the exact test of Hardy-Weinberg proportion for multiple alleles. *Biometrics*, **48**, 361–372.

Hasselman DJ, Ricard D, Bentzen P (2013) Genetic diversity and differentiation in a wide ranging anadromous fish, American shad (*Alosa sapidissima*), is correlated with latitude. *Molecular Ecology*, **22**, 1558–1573.

Hedgecock D, Barber PH, Edmands S (2007) Genetic approaches to measuring connectivity. *Oceanography*, **20**, 70–79.

Hedrick PW (2005) A standardized genetic differentiation measure. *Evolution*, **59**, 1633–1638.

Honnay O, Jacquemyn H, Nackaerts K, Breyne P, van Looy K (2010) Patterns of population genetic diversity in riparian and aquatic plant species along rivers. *Journal of Biogeography*, **37**, 1730–1739.

Hughes AR, Inouye BD, Johnson MTJ, Underwood N, Vellend M (2008) Ecological consequences of genetic diversity. *Ecology Letters*, **11**, 609–623.

Hung KH, Chiang TY, Chiu CT, Hsu TW, Ho CW (2009) Isolation and characterization of microsatellite loci from a potential biofuel plant *Miscanthus sinensis* (Poaceae). *Conservation Genetics*, **10**, 1377–1380.

Imbert E, Lefèvre F (2003) Dispersal and gene flow of *Populus nigra* (Salicaceae) along a dynamic river system. *Journal of Ecology*, **91**, 447–456.

Jørgensen U, Schwarz KU (2000) What do basic research? A lesson from commercial exploitation of *Miscanthus*. *New Phytologist*, **148**, 190–193.

Jost L (2008) G_{ST} and its relatives do not measure differentiation. *Molecular Ecology*, **17**, 4015–4026.

Li X, Hu D, Luo M *et al.* (2013) Nuclear DNA content variation of three *Miscanthus* species in China. *Genes & Genomics*, **35**, 13–20.

Liu W, Sang T (2013) Potential productivity of the *Miscanthus* energy crop in the Loess Plateau of China under climate change. *Environmental Research Letters*, **8**, 044003.

Liu Y, Wang Y, Huang H (2006) High interpopulation genetic differentiation and unidirectional linear migration patterns in *Myricaria laxiflora* (Tamaricaceae), an endemic riparian plant in the Three Gorges Valley of the Yangtze River. *American Journal of Botany*, **93**, 206–215.

Liu W, Yan J, Li J, Sang T (2012) Yield potential of *Miscanthus* energy crops in the Loess Plateau of China. *Global Change Biology Bioenergy*, **4**, 545–554.

Liu W, Mi J, Song Z, Yan J, Li JQ, Sang T (2014) Long-term water balance and sustainable production of *Miscanthus* energy crops in the Loess Plateau of China. *Biomass and Bioenergy*, **62**, 47–57.

Lowe WH, Allendorf FW (2010) What can genetics tell us about population connectivity? *Molecular Ecology*, **19**, 3038–3051.

Luikart G, Allendorf FW, Cornuet JM, Sherwin WB (1998) Distortion of allele frequency distributions provides a test for recent population bottlenecks. *Journal of Heredity*, **89**, 238–247.

Mable BK, Adam A (2007) Patterns of genetic diversity in outcrossing and selfing populations of *Arabidopsis lyrata*. *Molecular Ecology*, **16**, 3565–3580.

Manel S, Holderegger R (2013) Ten years of landscape genetics. *Trends in Ecology & Evolution*, **28**, 614–621.

Manel S, Schwartz MK, Luikart G, Taberlet P (2003) Landscape genetics: combining landscape ecology and population genetics. *Trends in Ecology & Evolution*, **18**, 189–197.

Manni F, Guerard E, Heyer E (2004) Geographic patterns of (genetic, morphologic, linguistic) variation: How barriers can be detected by using Monmonier's algorithm. *Human Biology*, **76**, 173–190.

Markert J, Champlin D, Gutjahr-Gobell R *et al.* (2010) Population genetic diversity and fitness in multiple environments. *BMC Evolutionary Biology*, **10**, 205.

Medrano M, Herrera CM (2008) Geographical structuring of genetic diversity across the whole distribution range of *Narcissus longispathus*, a habitat-specialist, mediterranean narrow endemic. *Annals of Botany*, **102**, 183–194.

Meeuwig MH, Guy CS, Kalinowski ST, Fredenberg WA (2010) Landscape influences on genetic differentiation among bull trout populations in a stream-lake network. *Molecular Ecology*, **19**, 3620–3633.

Mi J, Liu W, Yang W, Yan J, Li JQ, Sang T (2014) Carbon sequestration by *Miscanthus* energy crops plantations in a broad range semi-arid marginal land in China. *Science of Total Environment*, **496**, 373–380.

Murphy MA, Dezzani R, Pilliod DS, Storfer A (2010) Landscape genetics of high mountain frog metapopulations. *Molecular Ecology*, **19**, 3634–3649.

Nei M, Tajima F, Tateno Y (1983) Accuracy of estimated phylogenetic trees from molecular-data.II. Gene-frequency data. *Journal of Molecular Evolution*, **19**, 153–170.

Orsini L, Vanoverbeke J, Swillen I, Mergeay J, De Meester L (2013) Drivers of population genetic differentiation in the wild: isolation by dispersal limitation, isolation by adaptation and isolation by colonization. *Molecular Ecology*, **22**, 5983–5999.

Paetkau D, Calvert W, Stirling I, Strobeck C (1995) Microsatellite analysis of population structure in Canadian polar bears. *Molecular Ecology*, **4**, 347–354.

Paetkau D, Slade R, Burden M, Estoup A (2004) Genetic assignment methods for the direct, real-time estimation of migration rate: a simulation-based exploration of accuracy and power. *Molecular Ecology*, **13**, 55–65.

Peakall ROD, Smouse PE (2006) Genalex 6: genetic analysis in Excel. Population genetic software for teaching and research. *Molecular Ecology Notes*, **6**, 288–295.

Piry S, Luikart G, Cornuet JM (1999) BOTTLENECK: A computer program for detecting recent reductions in the effective population size using allele frequency data. *Journal of Heredity*, **90**, 502–503.

Piry S, Alapetite A, Cornuet JM, Paetkau D, Baudouin L, Estoup A (2004) GENECLASS2: A software for genetic assignment and first-generation migrant detection. *Journal of Heredity*, **95**, 536–539.

Pollux BJA, Luteijn A, Van Groenendae JM, Ouborg NJ (2009) Gene flow and genetic structure of the aquatic macrophyte *Sparganium emersum* in a linear unidirectional river. *Freshwater Biology*, **54**, 64–76.

Pritchard JK, Stephens M, Donnelly P (2000) Inference of population structure using multilocus genotype data. *Genetics*, **155**, 945–959.

Rannala B, Mountain JL (1997) Detecting immigration by using multilocus genotypes. *Proceedings of the National Academy of Sciences of the United States of America*, **94**, 9197–9201.

Raymond M, Rousset F (1995) Genepop (version 1.2): Population genetics software for exact tests and ecumenicism. *Journal of Heredity*, **86**, 248–249.

Raymond L, Plantegenest M, Vialatte A (2013) Migration and dispersal may drive to high genetic variation and significant genetic mixing: the case of two agriculturally important, continental hoverflies (*Episyrphus balteatus* and *Sphaerophoria scripta*). *Molecular Ecology*, **22**, 5329–5339.

Reed DH, Frankham R (2003) Correlation between fitness and genetic diversity. *Conservation Biology*, **17**, 230–237.

Rico Y, Holderegger R, Boehmer HJ, Wagner HH (2014) Directed dispersal by rotational shepherding supports landscape genetic connectivity in a calcareous grassland plant. *Molecular Ecology*, **23**, 832–842.

Rosenberg NA (2004) DISTRUCT: a program for the graphical display of population structure. *Molecular Ecology Notes*, **4**, 137–138.

Sang T (2011) Toward the domestication of lignocellulosic energy crops: learning from food crop domesticationfree access. *Journal of Integrative Plant Biology*, **53**, 96–104.

Sang T, Zhu W (2011) China's bioenergy potential. *Global Change Biology Bioenergy*, **3**, 79–90.

Schleuning M, Becker T, Vadillo GP, Hahn T, Matthies D, Durka W (2011) River dynamics shape clonal diversity and genetic structure of an Amazonian understorey herb. *Journal of Ecology*, **99**, 373–382.

Slatkin M (1987) Gene flow and the geographic structure of natural-populations. *Science*, **236**, 787–792.

Slatkin M (1993) Isolation by distance in equilibrium and non-equilibrium populations. *Evolution*, **47**, 264–279.

Slatkin M, Barton NH (1989) A comparison of three indirect methods for estimating average levels of gene flow. *Evolution*, **43**, 1349–1368.

Smouse PE, Peakall R (1999) Spatial autocorrelation analysis of individual multiallele and multilocus genetic structure. *Heredity*, **82**, 561–573.

Somerville C, Youngs H, Taylor C, Davis SC, Long SP (2010) Feedstocks for lignocellulosic biofuels. *Science*, **329**, 790–792.

Song G, Yu L, Gao B *et al.* (2013) Gene flow maintains genetic diversity and colonization potential in recently range-expanded populations of an Oriental bird, the Light-vented Bulbul (*Pycnonotus sinensis*, Aves: Pycnonotidae). *Diversity & Distributions*, **19**, 1248–1262.

Sun Q, Lin Q, Yi ZL, Yang Z, Zhou F (2010) A taxonomic revision of *Miscanthus* s.l. (Poaceae) from China. *Botanical Journal of the Linnean Society*, **164**, 178–220.

Taylor ZS, Hoffman SMG (2014) Landscape models for nuclear genetic diversity and genetic structure in white-footed mice (*Peromyscus leucopus*). *Heredity*, **112**, 588–595.

Van Oosterhout C, Hutchinson WF, Wills DPM, Shipley P (2004) MICRO-CHECKER: software for identifying and correcting genotyping errors in microsatellite data. *Molecular Ecology Notes*, **4**, 535–538.

Vasemägi A (2006) The adaptive hypothesis of clinal variation revisited: single-locus clines as a result of spatially restricted gene flow. *Genetics*, **173**, 2411–2414.

Verhoeven KJF, Macel M, Wolfe LM, Biere A (2011) Population admixture, biological invasions and the balance between local adaptation and inbreeding depression. *Proceedings of the Royal Society B: Biological Sciences*, **278**, 2–8.

Vähä JP, Erkinaro J, NiemelÄ E, Primmer CR (2007) Life-history and habitat features influence the within-river genetic structure of Atlantic salmon. *Molecular Ecology*, **16**, 2638–2654.

Vrijenhoek RC (2010) Genetic diversity and connectivity of deep-sea hydrothermal vent metapopulations. *Molecular Ecology*, **19**, 4391–4411.

Wang IJ (2012) Environmental and topographic variables shape genetic structure and effective population sizes in the endangered Yosemite toad. *Diversity and Distribution*, **18**, 1033–1041.

Wang R, Compton SG, Chen XY (2011) Fragmentation can increase spatial genetic structure without decreasing pollen-mediated gene flow in a wind-pollinated tree. *Molecular Ecology*, **20**, 4421–4432.

Wei X, Meng H, Jiang M (2013) Landscape genetic structure of a streamside tree species *Euptelea pleiospermum* (Eupteleaceae): contrasting roles of river valley and mountain ridge. *PLoS One*, **8**, e66928.

Weigel D, Connolly P, Powell M (2013) The impact of small irrigation diversion dams on the recent migration rates of steelhead and redband trout (*Oncorhynchus mykiss*). *Conservation Genetics*, **14**, 1255–1267.

Weir BS, Cockerham CC (1984) Estimating *F*-statistics for the analysis of population structure. *Evolution*, **38**, 1358–1370.

Wright S (1969) *Evolution and the Genetics of Populations, Vol. 2: The Theory of Gene Frequencies*. University Chicago Press, Chicago, IL.

Xu Q, Xing S, Zhu C *et al.* (2015) Population transcriptomics reveals a potentially positive role of expression diversity in adaptation. *Journal of Integrative Plant Biology*, **3**, 284–299.

Yan J, Chu HJ, Wang HC, Li JQ, Sang T (2009) Population genetic structure of two *Medicago* species shaped by distinct life form, mating system and seed dispersal. *Annals of Botany*, **103**, 825–834.

Yan J, Chen W, Luo F *et al.* (2012) Variability and adaptability of *Miscanthus* species evaluated for energy crop domestication. *Global Change Biology Bioenergy*, **4**, 49–60.

Yan J, Zhu CY, Liu W *et al.* (2015) High photosynthetic rate and water use efficiency of *Miscanthus lutarioriparius* characterize an energy crop in the semiarid temperate region. *Global Change Biology Bioenergy*, **7**, 207–218.

Yang Z, Wang H, Saito Y *et al.* (2006) Dam impacts on the Changjiang (Yangtze) River sediment discharge to the sea: the past 55 years and after the Three Gorges Dam. *Water Resource Research*, **42**, W04407.

Zhou HF, Li SS, Ge S (2011) Development of microsatellite markers for *Miscanthus sinensis* (Poaceae) and cross-amplification in other related species. *American Journal of Botany*, **98**, e195–e197.

Zhou HF, Li SS, Ge S (2013) Isolation and characterization of microsatellite loci for a bioenergy grass, *Miscanthus sacchariflorus* (Poaceae). *Applications in Plant Sciences*, **1**, 1200210.

Supporting Information

Additional Supporting Information may be found in the online version of this article:

Table S1. Comparison of the genetic diversity found at 16 microsatellite loci in *Miscanthus lutarioriparius*.
Table S2. Pairwise estimates of F_{ST} (below diagonal) and D_{est} (above diagonal) between populations.
Figure S1. The percentage of individuals per population assigned to some populations by assignment test.

